Hindawi
Advances in High Energy Physics
Volume 2018, Article ID 4174602, 7 pages
https://doi.org/10.1155/2018/4174602

Research Article

Predictions for the Isolated Diphoton Production through NNLO in QCD and Comparison to the 8 TeV ATLAS Data

Bouzid Boussaha, Farida Iddir, and Lahouari Semlala

Laboratoire de Physique Théorique d'Oran (LPTO), University of Oran1-Ahmed Ben Bella, BP 1524, El M'nouar Oran 31000, Algeria

Correspondence should be addressed to Lahouari Semlala; semlala.lahouari@univ-oran.dz

Received 27 March 2018; Revised 18 June 2018; Accepted 18 July 2018; Published 7 August 2018

Academic Editor: Juan José Sanz-Cillero

We present cross-section predictions for the isolated diphoton production in next-to-next-to-leading order (NNLO) QCD using the computational framework MATRIX. Both the integrated and the differential fiducial cross-sections are calculated. We found that the arbitrary setup of the isolation procedure introduces uncertainties with a size comparable to the estimation of the theoretical uncertainties obtained with the customary variation of the factorization and renormalization scales. This fact is taken into account in the final result.

1. Introduction

Considerable attention, both experimental and theoretical, has been paid to the study of the diphoton productions. This process is relevant for testing the standard model predictions and is of great importance in Higgs studies. The diphoton final state is also important in new physics researches: the extra-dimensions, the supersymmetry, and the new heavy resonances are three important topics among others.

The theoretical calculations are possible thanks to the codes DIPHOX [1], ResBos [2], 2gRes [3], 2gNNLO [4], MCFM [5], and recently MATRIX [6].

In addition to the *direct* production from the hard subprocess, photons can also result from the fragmentation subprocesses of QCD partons. The complete NLO one- and two-*fragmentation* contributions are implemented in DIPHOX. In ResBos only a simplified one-fragmentation contribution is considered but the resummation of initial-state gluon radiation to NNLL accuracy is included. Both DIPHOX and ResBos implement the gg $\longrightarrow \gamma\gamma$ component, to LO and NLO in QCD, respectively. In the (NLO) MCFM calculations, the fragmentation component is implemented to LO accuracy.

Thanks to the high rate of production of final diphoton pairs (considered as relatively clean), experimentalists make precise measurements, pushing the experimental uncertainties down to the percent level; thus, NLO calculations have become insufficient and therefore more precise investigations are required in order to reproduce the data and to provide a precise modeling of the SM backgrounds.

During the first run of the LHC (Run I), measurements of the production cross-section for two isolated photons at a center-of-mass energy of $\sqrt{s}$ = 7 TeV are performed by ATLAS [7] and CMS [8], based on an integrated luminosity of 4.9 fb^{-1} and 5.0 fb^{-1}, respectively. This is concluded by ATLAS [9] at $\sqrt{s}$ = 8 TeV using an integrated luminosity of 20.2 fb^{-1} which gives a much more accurate result.

In [9], the authors reported that NLO calculations fail to reproduce the data and even if there is improvement of the result with 2gNNLO, it remains insufficient.

Although the NNLO isolated diphoton production cross-sections can be calculated using the 2gNNLO and MCFM public codes, we used the most recent code MATRIX, because, in addition to its NNLO accuracy, it allows us to estimate systematic errors related to the q_T-subtraction procedure in an automatic way (see below).

Our work is organized as follows. In Section 2.1, we give a short description of the MATRIX code. In Section 2.2, we present the two isolation prescriptions used in the analysis. We propose a precise estimation of the uncertainties in

NNLO QCD calculations containing at least one photon in the final state. In Section 2.3, the NNLO cross-section results are presented and compared to LHC data. We finish with the conclusion in Section 3.

2. NNLO Cross-Sections

2.1. The MATRIX Code. The parton-level Monte Carlo generator MATRIX performs fully differential computations at the next-to-next-to-leading order (NNLO) QCD; it is based on a number of different computations and tools from various people and groups [6, 10–15]. It achieves NNLO accuracy by using the q_T-subtraction formalism in combination with the Catani–Seymour dipole subtraction method. The systematic uncertainties inherent to the q_T-subtraction procedure may be controlled down to the few per mille level or better for all NNLO predictions. To do this, a dimensionless cut-off r_{cut} is introduced which renders all cross-section pieces separately finite and the power-suppressed contributions vanish in the limit $r_{cut} \longrightarrow 0$. MATRIX simultaneously computes the cross-section at several r_{cut} values and then the extrapolated result is evaluated, including an estimate of the uncertainty of the extrapolation procedure, in an automatic way.

We can apply realistic fiducial cuts directly on the phase-space. The core of MATRIX framework is MUNICH Monte Carlo program, allowing us to compute both QCD and EW corrections at NLO accuracy. The loop-induced gg contribution entering at the NNLO is available for the diphoton production process.

2.2. Isolation Parameters. An isolation requirement is necessary to prevent contamination of the photons by hadrons produced during the collision, arising from the decays of π^0, η, etc. Two prescriptions may be used for this purpose:

(i) The standard cone isolation criterion, used by collider experiments: a photon is assumed to be isolated if the amount of deposited hadronic transverse energy $\sum_h E_T^h$ is smaller than some value $E_T^{\max}$, inside the cone of radius R in azimutal ϕ and rapidity y angle centered around the photon direction:

$$\sum_h E_T^h \leq E_T^{\max}, \qquad r = \sqrt{\left(\phi - \phi_\gamma\right)^2 + \left(y - y_\gamma\right)^2} \leq R. \tag{1}$$

$E_T^{\max}$ can be either a fixed value or a fraction ε of the transverse momentum of the photon p_T^γ:

$$E_T^{\max} = \text{const.} \quad \text{or} \quad E_T^{\max} = \varepsilon p_T^\gamma, \quad 0 < \varepsilon \leq 1. \tag{2}$$

R and $E_T^{\max}$ are chosen by the experiment; ATLAS and CMS use $R = 0.4$, but $E_T^{\max}$ differs in their various measurements:

(ii) The "smooth" cone or Frixione isolation criterion [16]: in this case $E_T^{\max}$ is multiplied by a function $\chi(r)$ such that

$$\lim_{r \longrightarrow 0} \chi(r) = 0, \qquad 0 < \chi(r) < 1 \quad \text{if } 0 < r < R; \tag{3}$$

a possible (and largely used) choice is

$$\chi(r) = \left[\frac{1 - \cos(r)}{1 - \cos(R)}\right]^n \tag{4}$$

so that

$$\sum_h E_T^h \leq \chi \left[\frac{1 - \cos(r)}{1 - \cos(R)}\right]^n E_T^{\max}, \qquad r = \sqrt{\left(\phi - \phi_\gamma\right)^2 + \left(y - y_\gamma\right)^2} \leq R, \qquad (\text{typically } n = 1). \tag{5}$$

Despite the fact that the Frixione criterion (formally) eliminates all fragmentation contribution, it is not yet included in the experimental studies. On the other hand, the use of this criterion by the theoretical investigations at NNLO is necessary to ensure an Infra-Red (IR) safe definition of the cross-section since no fragmentation functions are included.

In ATLAS measurement [9], the standard criterion is adopted for DIPHOX and ResBos but the "smooth" prescription is used for 2gNNLO, assuming $E_T^{\max} = 11\ GeV$. This is far from the Les Houches accord 2013 recommendations which state that to match experimental conditions to theoretical calculations with reasonable accuracy, the isolation parameters must be tight enough: $E_T^{\max} \leq 5\ GeV$ or $\varepsilon < 0.1$ (assuming $n = 1$) [17].

In [18], the authors presented a rather complete study of the impact of the isolation parameters on the diphoton cross-sections. We can lift the following points from this study:

(i) The NNLO cross-sections are more sensitive to the variation of the parameters of isolation in comparison with the NLO results.

(ii) At fixed $n = 1$, the total NNLO cross-section for the "smooth" isolation increases by 6% in going from $E_T^{\max} = 2$ to 10 GeV.

(iii) Considering the interval $0.5 < n < 2$, at fixed $E_T^{\max} = 4$ GeV, the total NNLO cross-section with $n = 1$ increases by about 4% with $n = 0.5$ and decreases by about 5% with $n = 2$; the corresponding scale uncertainty is less than ±8.7%.

We notice that the isolation uncertainties due to the choice of the isolation parameters are comparable to the scale uncertainties; thus, we have to consider the arbitrary choice of these parameters as a major source of the theoretical systematic errors as well as uncertainties related to the choice of the scale. This must be included in the final result.

To evaluate these isolation uncertainties (i.e., to determine both the central value and deviations), we use MATRIX to calculate the NLO integrated cross-sections by varying the parameters n =0.1, 0.5, 1, 2, 4, 10 and $E_T^{\max} = 2, 3, 4, 5, 8, 11$GeV; then the results are compared to the NLO cross-sections obtained by running the DIPHOX code using the standard isolation prescription with the same $E_T^{\max}$ and R parameters.

The so-called box (NNLO) contribution to the channel $gg \longrightarrow \gamma\gamma$ is removed from the DIPHOX results to ensure that the comparison holds at the same NLO-order and the fine structure constant α is fixed to $1/137$; the setup is summarized in Table 1 and results are shown in Figures 1-2.

To minimize the difference between the isolation definitions used in the theoretical and the experimental analyses, the central value σ^{NLO} is determined at the value $n = n_0$ so that

$$\sigma^{\mathrm{NLO}} \equiv \left(\sigma^{\mathrm{NLO}}_{\mathrm{MATRIX}}\right)_{n=n_0} \simeq \sigma^{\mathrm{NLO}}_{\mathrm{DIPHOX}}, \tag{6}$$

$$\left(R \text{ and } E_T^{\max} \text{ are fixed according to the isolation experimental requirement}\right); \tag{7}$$

The isolation uncertainties are evaluated by varying n from $\sim (1/2)n_0$ to $\sim 2n_0$. This procedure is adopted in our NNLO calculations (see Section 2.3).

The "central value" of the parameter $n = n_0$ depends on the value of $E_T^{\max}$ (see Table 2); this is consistent with the results of [18].

2.3. NNLO Results and Comparison with Data. We consider proton-proton collisions at the 8 TeV LHC. We choose the invariant mass of the photon pair at the central scale, i.e.,

$$\mu = m_{\gamma\gamma} < 1700\ GeV. \tag{8}$$

the Frixione isolation with $0.5 < n < 2$, $E_T^{\max} = 11$ GeV, and $R = 0.4$ (see (5)), and the following fiducial cuts:

$$\begin{aligned} p_T^{\gamma_1} &> 40\ GeV, \\ p_T^{\gamma_2} &> 30\ GeV, \\ \left|\eta^{\gamma}\right| &< 2.37; \end{aligned} \tag{9}$$

excluding the gap region

$$1.37 < \left|\eta^{\gamma}\right| < 1.56. \tag{10}$$

The experimental angular separation between the photons is set to

$$R_{\gamma\gamma} = \sqrt{\left(y_1 - y_2\right)^2 + \left(\phi_1 - \phi_2\right)^2} > 0.4, \tag{11}$$

we have

$$\begin{aligned} &\cosh\left(y_1 - y_2\right) - \cos\sqrt{R_{\gamma\gamma}^2 - \left(\phi_1 - \phi_2\right)^2} \\ &\geq \left[\cosh\left(y_1 - y_2\right) - \cos\sqrt{0.4^2 - \left(\phi_1 - \phi_2\right)^2}\right]_{\min} \\ &\simeq 0.08, \end{aligned} \tag{12}$$

and then

$$\left(m_{\gamma\gamma}\right)_{\min} = \sqrt{2\left(p_T^{\gamma_1}\right)_{\min}\left(p_T^{\gamma_2}\right)_{\min}\left[\cosh\left(y_1 - y_2\right) - \cos\sqrt{R_{\gamma\gamma}^2 - \left(\phi_1 - \phi_2\right)^2}\right]_{\min}} \simeq 13.7\ \mathrm{GeV}. \tag{13}$$

The appropriate value of the fine structure constant α is the value of the electromagnetic coupling at the invariant mass final state $m_{\gamma\gamma}$, and since $m_{\gamma\gamma} > 0$, a value such as $\alpha_{\mathrm{e.m.}}(\mu = M_Z)$ might be more appropriate than $\alpha_{\mathrm{e.m.}}(\mu = 0) \simeq 1/137$. Then α is fixed to $1/128.9$.

Several modern NNLO PDF sets are used (CT14 [21], MMHT14 [22], and NNPDF3.1 [23]); the evolution of α_s at 3-loop order is provided by the corresponding PDF set.

For CT14, the central value of the NNLO integrated fiducial cross-section is evaluated at the isolation parameters ($n = n_0 = 0.84$, $E_T^{\max} = 11 GeV$) within the scale choice $\mu_R = \mu_F = m_{\gamma\gamma}$(central scale):

$$\left(\sigma^{\mathrm{fid}}_{\mathrm{tot}}\right)^{\mathrm{NNLO}}_{n=0.84} = 15.60 \pm 0.09\ (\mathrm{num})\ \ \mathrm{pb}, \tag{14}$$

calculated at r_{cut} extrapolated to zero.

The scale uncertainties are estimated in the usual way by independently varying μ_R and μ_F in the range

$$\begin{aligned} \frac{1}{2} m_{\gamma\gamma} &\leq \mu_R, \\ \mu_F &\leq 2 m_{\gamma\gamma}, \end{aligned} \tag{15}$$

with the constraint

$$\frac{1}{2} \leq \frac{\mu_R}{\mu_F} \leq 2. \tag{16}$$

The relative scale uncertainty in the integrated cross-section is $\left({}^{+6.7\%}_{-5.6\%}\right)$.

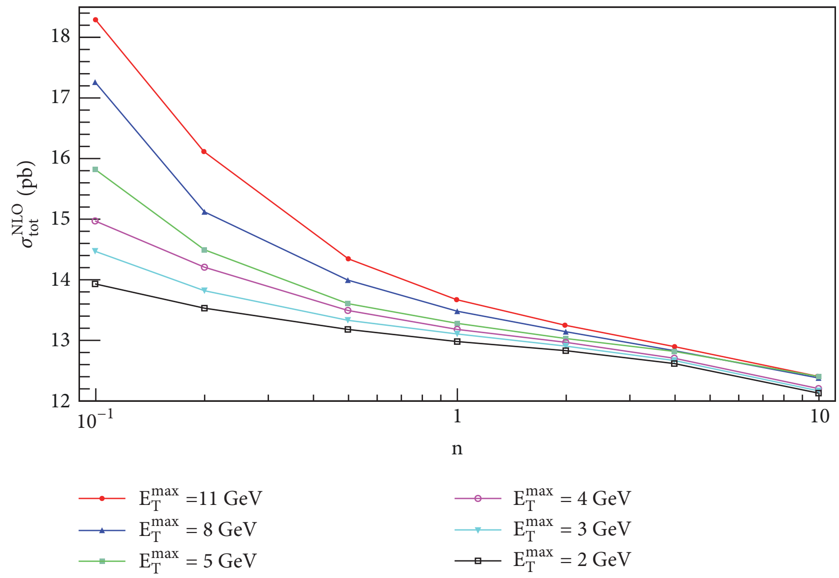

FIGURE 1: The MATRIX integrated fiducial cross-section σ_{tot}^{NLO} as a function of the parameter n related to Frixione isolation criterion (see (5)) for different values of E_T^{max}.

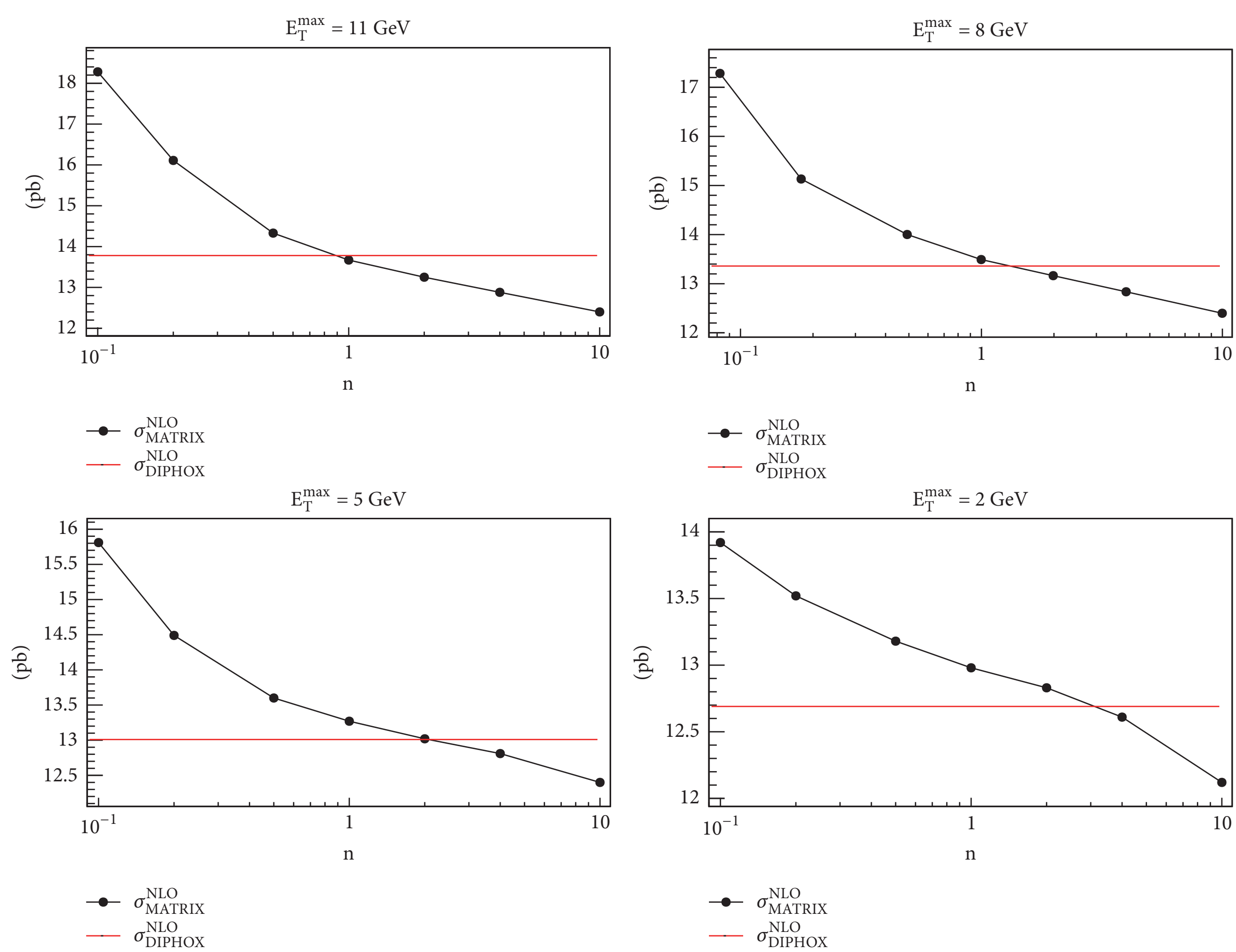

FIGURE 2: The MATRIX and the DIPHOX integrated fiducial cross-section σ_{tot}^{NLO} as a function of the parameter n related to Frixione isolation criterion (see (5)) for several values of E_T^{max}. The "central values" of the parameter $n = n_0$ depend on the value of E_T^{max}; they are reported in Table 2.

Table 1: Setup of the diphoton production process used in the NLO runs.

DIPHOX v.1.2	MATRIX v.1.0
Pdf [19]: cteq6	cteq6
α fixed to 1/137	α fixed to 1/137
$p_T^{\gamma} > 25\ GeV,\ \lvert\eta^{\gamma}\rvert < 2.37$;	$p_T^{\gamma} > 25\ GeV,\ \lvert\eta^{\gamma}\rvert < 2.37$;
$80 < m_{\gamma\gamma} < 1700$ GeV	$80 < m_{\gamma\gamma} < 1700$ GeV
isolation: $R = 0.4$, standard, E_T^{max}.	$R = 0.4$, "smooth", (E_T^{max}, n)
fragmentation functions [20]: BFG set II	-
The direct part: born only, no box contributions	-

Table 2: The "central values" of the parameter $n = n_0$.

E_T^{max}(GeV)	n_0	σ^{NLO}_{MATRIX}(pb)
11	0.84	$13.78 \pm 0.12(\text{num})^{+6.1\%}_{-5.0\%}(\text{scale})$
8	1.2	$13.36 \pm 0.10(\text{num})^{+5.9\%}_{-4.8\%}(\text{scale})$
5	2.0	$13.01 \pm 0.10(\text{num})^{+5.8\%}_{-4.7\%}(\text{scale})$
2	3.2	$13.69 \pm 0.11(\text{num})^{+5.7\%}_{-4.6\%}(\text{scale})$

The relative isolation uncertainty (at the central scale) is calculated by varying n from 0.5 to 2:

$$\begin{aligned} \frac{\sigma_{n=0.5} - \sigma_{n=0.84}}{\sigma_{n=0.84}} &\simeq +3.8\% \\ \frac{\sigma_{n=2} - \sigma_{n=0.84}}{\sigma_{n=0.84}} &\simeq -5.5\% \end{aligned} \tag{17}$$

The impact of the variation of the strong coupling constant is also investigated. The change of $\alpha_s(M_Z^2)$ by ± 0.001 from the central value 0.118 leads to variations $\left(^{+0.6\%}_{-1.0\%}\right)$ in the fiducial integrated cross-section. The cross-sections related to CT14, MMHT14, and NNPDF3.1 modern PDF sets are very close to each other with an uncertainty less than 0.4%.

We can write our theoretical prediction of the integrated fiducial cross-section as:

$$\begin{aligned} \sigma^{\text{fid}}_{\text{tot}} &\simeq 15.60 \pm 0.09\,(\text{num}) \begin{matrix} +6.7\% \\ -5.7\% \end{matrix}\,(\text{scale}) \begin{matrix} +3.8\% \\ -5.5\% \end{matrix}\,(\text{iso}) \\ &\simeq 15.60 \pm 0.09\,(\text{num}) \begin{matrix} +1.05 \\ -0.89 \end{matrix}\,(\text{scale}) \begin{matrix} +0.59 \\ -0.86 \end{matrix}\,(\text{iso}) \\ &\simeq 15.60^{+1.21}_{-1.24} \simeq (15.6 \pm 1.2)\ \text{pb} \end{aligned} \tag{18}$$

which is consistent with the experimental data [9]: (16.8 ± 0.8)pb.

Note that the theoretical uncertainties are dominated by both the scale and the isolation systematic errors which are of the same order.

Since this process involves isolated photons in the final state it has a relatively large numerical uncertainty at NNLO after the $r_{cut} \longrightarrow 0$ extrapolation, and as recommended by authors of [6], the distribution calculated at fixed $r_{cut} = 0.05\%$ must be multiplied by the correction factor:

$$\frac{\left(\sigma^{\text{fid}}_{\text{tot}}\right)_{r_{cut}\longrightarrow 0}}{\left(\sigma^{\text{fid}}_{\text{tot}}\right)_{r_{cut}=0.05\%}}\ (\sim 0.98)\,. \tag{19}$$

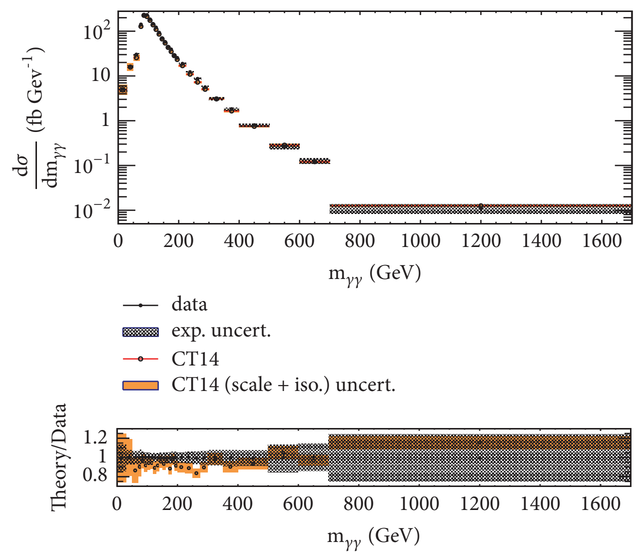

Figure 3: The MATRIX differential fiducial cross-section related to CT14 as a function of $m_{\gamma\gamma}$ compared to the data [9].

The MATRIX differential cross-section is consistent with data as shown in Figures 3-4.

3. Conclusion

We presented the calculation of the integrated and differential cross-sections for the isolated diphoton production in pp collisions at the center–of–mass energy $\sqrt{s} = 8$ TeV in next-to-next-to-leading order (NNLO) QCD using the computational framework MATRIX. A special care was paid to the choice of the Frixione isolation parameters. We kept the same value of $E_T^{max} = 11\ GeV$ and $R = 0.4$ used by experimentalists but we adjusted the value of the parameter n until the integrated cross-section calculated by MATRIX matches that calculated by DIPHOX at the same NLO-order (without the *Box*-contribution to the channel $gg \longrightarrow \gamma\gamma$).

Once these parameters were fixed, we calculated the central value of the MATRIX (NNLO) cross-sections and by varying the Frixione parameter n from 0.5 to 2, we estimated the relative isolation uncertainty $\left(^{+3.8\%}_{-5.5\%}\right)$. The scale uncertainty is found to be equal to$\left(^{+6.7\%}_{-5.7\%}\right)$.

Both the scale and the isolation uncertainties were of the same order and represent the main source of the theoretical errors; the uncertainties inherent to the q_T-subtraction procedure ($\sim$ 0.6%) and to the variation of the coupling constant $\alpha_s(M_Z^2)$ ($\sim$ 0.8%) were negligible.

Our predictions for the differential and the integrated cross sections are in good agreement with the data. In

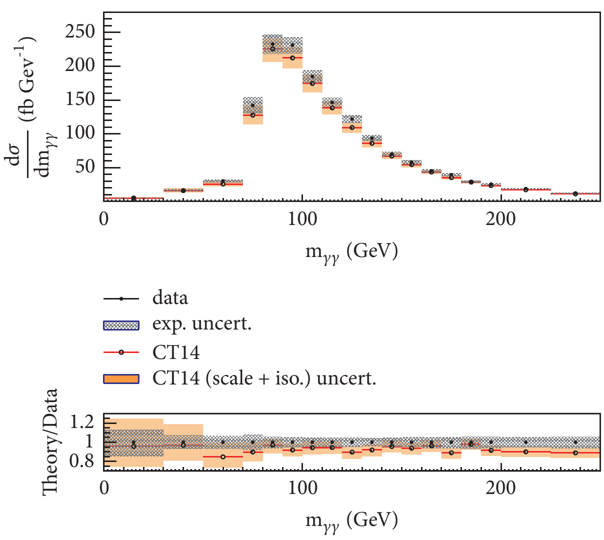

Figure 4: The MATRIX differential fiducial cross-section related to CT14 as a function of $m_{\gamma\gamma}$ compared to the data [9], in the range $0 < m_{\gamma\gamma} < 250$ *GeV*.

particular, we have $\sigma_{\mathrm{tot}}^{\mathrm{fid}} \simeq 15.60 \pm 0.09\ (\mathrm{num})\ {}^{+6.7\%}_{-5.7\%}\ (\mathrm{scale})\ {}^{+3.8\%}_{-5.5\%}\ (\mathrm{iso}) \simeq (15.6 \pm 1.2)$ pb.

Data Availability

The data used to support the findings of this study are available from the corresponding author upon request.

Conflicts of Interest

The authors declare that they have no conflicts of interest.

Acknowledgments

This work was realized with the support of the FNR (Algerian Ministry of Higher Education and Scientific Research), as part of the research Project D018 2014 0044. The authors gratefully acknowledge computing support provided by the Research Center on Scientific and Technical Information (CERIST) in Algiers (Algeria) through the HPC Platform IBNBADIS.

References

[1] T. Binoth, J. P. Guillet, E. Pilon, and M. Werlen, "A full next-to-leading order study of direct photon pair production in hadronic collisions," *The European Physical Journal C*, vol. 16, p. 311, 2000.

[2] C. Balazs, E. L. Berger, P. M. Nadolsky, and C.-P. Yuan, "Gluon-gluon contributions to the production of continuum diphoton pairs at hadron colliders," *Physical Review D*, vol. 76, Article ID 013008, 2007.

[3] L. Cieri, F. Coradeschi, and D. de Florian, "Diphoton production at hadron colliders: transverse-momentum resummation at next-to-next-to-leading logarithmic accuracy," *Journal of High Energy Physics*, vol. 2015, no. 6, 2015.

[4] S. Catani, L. Cieri, D. de Florian, G. Ferrera, and M. Grazzini, "Diphoton production at hadron colliders: a fully differential QCD calculation at next-to-next-to-leading order," *Physical Review Letters*, vol. 108, no. 8, Article ID 072001, 2012.

[5] R. Boughezal, J. M. Campbell, R. K. Ellis et al., "Color-singlet production at NNLO in MCFM," *The European Physical Journal C*, vol. 77, no. 1, 2017.

[6] M. Grazzini, S. Kallweit, and M. Wiesemann, "Fully differential NNLO computations with MATRIX," https://arxiv.org/abs/1711.06631.

[7] ATLAS Collaboration, "Measurement of isolated-photon pair production in pp collisions at $\sqrt{s} = 7$ TeV with the ATLAS detector," *Journal of High Energy Physics*, vol. 2013, p. 086, 2013.

[8] CMS Collaboration, "Measurement of differential cross sections for the production of a pair of isolated photons in pp collisions at $\sqrt{s} = 7$ TeV," *The European Physical Journal C*, vol. 74, p. 3129, 2014.

[9] ATLAS Collaboration, "Measurements of integrated and differential cross sections for isolated photon pair production in pp collisions at $\sqrt{s} = 8$ TeV with the ATLAS detector," *Physical Review D*, vol. 95, Article ID 112005, 2017.

[10] C. Anastasiou, E. W. Nigel Glover, and M. E. Tejeda-Yeomans, "Two-loop QED and QCD corrections to massless fermion-boson scattering," *Nuclear Physics B*, vol. 629, no. 1–3, pp. 255–289, 2002.

[11] F. Cascioli, P. Maierhöfer, and S. Pozzorini, "Scattering Amplitudes with Open Loops," *Physical Review Letters*, vol. 108, no. 11, 2012.

[12] S. Catani, L. Cieri, D. de Florian, G. Ferrera, and M. Grazzini, "Diphoton production at hadron colliders: a fully differential QCD calculation at next-to-next-to-leading order," *Physical Review Letters*, vol. 117, no. 8, 2016.

[13] S. Catani, L. Cieri, D. de Florian, G. Ferrera, and M. Grazzini, "Vector-boson production at hadron colliders: hard-collinear coefficients at the NNLO," *The European Physical Journal C*, vol. 72, no. 11, pp. 1–9, 2012.

[14] S. Catani and M. Grazzini, "Next-to-next-to-leading-order subtraction formalism in hadron collisions and its application to higgs-boson production at the large hadron collider," *Physical Review Letters*, vol. 98, no. 22, 2007.

[15] A. Denner, S. Dittmaier, and L. Hofer, "COLLIER: A fortran-based complex one-loop library in extended regularizations," *Computer Physics Communications*, vol. 212, pp. 220–238, 2017.

[16] S. Frixione, "Isolated photons in perturbative QCD," *Physics Letter B*, vol. 429, Article ID 9801442, p. 369, 1998.

[17] L. Cieria, "Diphoton isolation studies," https://arxiv.org/abs/1510.06873.

[18] S. Catani, L. Cieri, D. de Florian, G. Ferrera, and M. Grazzini, "Diphoton production at the LHC: a QCD study up to NNLO," *Journal of High Energy Physics*, vol. 2018, p. 142, 2018.

[19] J. Pumplin, D. R. Stump, J. Huston, H.-L. Lai, P. Nadolsky, and W.-K. Tung, "New generation of Parton distributions with uncertainties from global QCD analysis," *Journal of High Energy Physics*, vol. 2002, p. 012, 2002.

[20] L. Bourhis, M. Fontannaz, and J. P. Guillet, "Quark and gluon fragmentation functions into photons," *The European Physical Journal C*, vol. 2, no. 3, pp. 529–537, 1998.

[21] S. Dulat, T.-J. Hou, J. Gao et al., "New parton distribution functions from a global analysis of quantum chromodynamics," *Physical Review D*, vol. 93, Article ID 033006, 2016.

[22] L. A. Harland-Lang, A. D. Martin, P. Motylinski, and R. S. Thorne, "Parton distributions in the LHC era: MMHT 2014 PDFs," *The European Physical Journal C*, vol. 75, article 204, 2015.

[23] The NNPDF Collaboration, "Parton distributions from high-precision collider data," https://arxiv.org/abs/1706.00428.